Analysis of the effectiveness of lightning and surge protection in a large solar farm

KONRAD SOBOLEWSKI [ID] [✉], EMILIA SOBIESKA [ID]

Warsaw University of Technology, Faculty of Electrical Engineering
Poland

e-mail: {✉konrad.sobolewski/emilia.sobieska.dokt}@pw.edu.pl

Abstract: The aim of the considerations presented in the article was a stand-alone ground-based photovoltaic power plant. The article is devoted to the qualitative analysis of some lightning protection configurations. These types of constructions often require an individual look at the design and execution of lightning protection installations, which causes problems with the selection of optimal solutions. These problems relate primarily to the way the lightning rods are arranged to create protection zones, but also to the way they are attached: to the supporting structure for PV modules or as free-standing. Another problem raised in the article is the way how lightning current is discharged from rods to the ground and how it is dispersed there. Due to the vast area of such facilities and the requirements for electrical safety, it is necessary to consider and design a ground system with optimal electrical parameters, but also technical and economic ones. All these elements have their impact on the value of voltages induced in the electrical installation, which is also presented in the content of the article as the magnetic field distribution and calculation of induced voltages in an exemplary configuration. Finally, this article will compare described technical solutions encountered in selecting the best protection method for this type of photovoltaic installation.

Key words: ANSYS simulations, electric safety, grounding system, magnetic field distribution, lightning modeling, lightning protection, photovoltaic power plant

1. Introduction

Photovoltaic systems are designed for a service life up to 30 years. Due to their exposed location, they are very often exposed to direct and indirect lightning at this time. One of the key parameter influences on the probability of the event is the lightning density factor. It is estimated that in Poland the number of stormy days ranges from 15 on the coast at the north to 33 in the

south-eastern regions of the country [1]. However, in other regions of the world, this density may be several times higher, which is due to the geographical location and local environmental conditions. Regarding the standardization requirements, it can be noted that this coefficient is calculated differently, resulting in differences in the results of the calculations [2]. Therefore, since the chances of a lightning event occurring are considerable, it should be considered to equip the facilities with a comprehensive lightning protection system [3], especially if it is an important object like a power plant. Its task is to protect against the effects of a direct lightning strike to elements of a photovoltaic installation and from the impact of voltages induced by a lightning electromagnetic pulse (LEMP) produced by lightning current. Due to various technical conditions protection may be implemented in multiple ways, which may affect the effectiveness of protection.

The specific construction and location of this type of object make the design of the lightning protection installation project a kind of challenge. Computer modeling and simulation can help to solve possible problems and dispel doubts. Modeling of lightning protection and overvoltage hazard is often made with circuit simulations [4], but field simulations may be more accurate by considering the geometry of the installation. In this situation, however, it is necessary to consider the adjustment of the size of the object, its environment and the calculating mesh. This is an important parameter due to the speed of calculations, but above all the accuracy of the results obtained.

2. Lightning hazard

The lightning hazard for free-standing photovoltaic installations results mainly from their exposed location and relatively large building area. Both of these factors lead to high probability values of a direct lightning strike, which may cause electrical, thermal and mechanical hazards to these objects. Due to the large size of the electrical installation and the high dynamics of lightning current, induced voltages can also reach significant values, exceeding the voltage strength of the attached devices or the insulation of the wires. The typical shape of a lightning discharge is shown in Fig. 1.
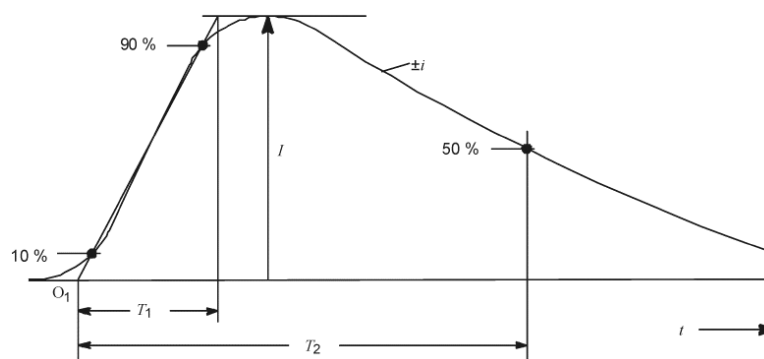

Fig. 1. Typical shape of lightning current: O_1 – contractual origin of surge, I – current peak value, T_1 – rise time, T_2 – time to half values of peak on tail [5]

Depending on the type of discharge (bottom-up or top-down), its polarization (positive or negative) and time positioning (first, subsequent or long-lasting), the above parameters will take different values, which are described in detail in the standard [5]. Typical impact time parameters used in the analysis of the effects of direct lightning discharge are $T_1 = 10$ µs and $T_2 = 350$ µs. As it can be seen, this is a very dynamic disturbance. For further calculations, a peak current value of $I = 40$ kA was used, which value corresponds statistically to the most often probability, and as time parameters for simulation in the direction of induced voltages in the worst case, which is a rise time of $T_1 = 0.25$ µs, corresponding to one of the subsequent discharges.

3. Methods of positioning and installation of lightning rods

Stand-alone photovoltaic power plants are usually located in open terrain, directly on the ground surface. The photovoltaic modules are mounted on supporting structures, commonly known as tables. They are made of welded steel profiles with sufficiently large cross-sections that meet the structural, mechanical requirements defined by the lightning protection standard [6]. An example of such a table is shown in Fig. 2. The supporting legs of the steel construction were plunged at 1.8 m depth into the ground, so the underground part became part of the grounding system.
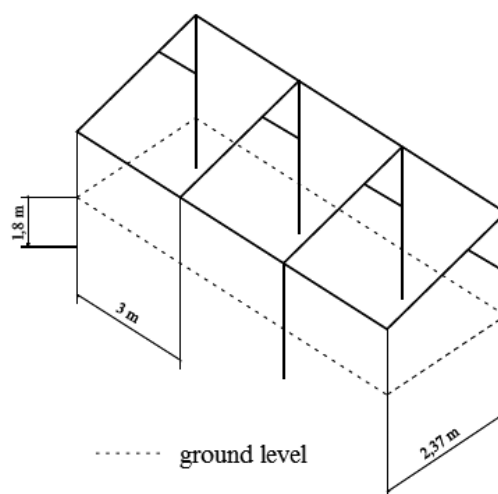

Fig. 2. Exemplary geometry of supporting construction for photovoltaic modules

Due to the vastness of the installation, the panels were placed on a certain number of tables, and each of them was galvanically connected with the adjacent ones in the row by equalizing connections (Fig. 3).

Lightning rods, which are part of the lightning protection system, are designed to locate the placement of the atmospheric discharge, hence they should be installed in the way to create a protection zone against direct lightning strikes. This zone should protect devices and installations
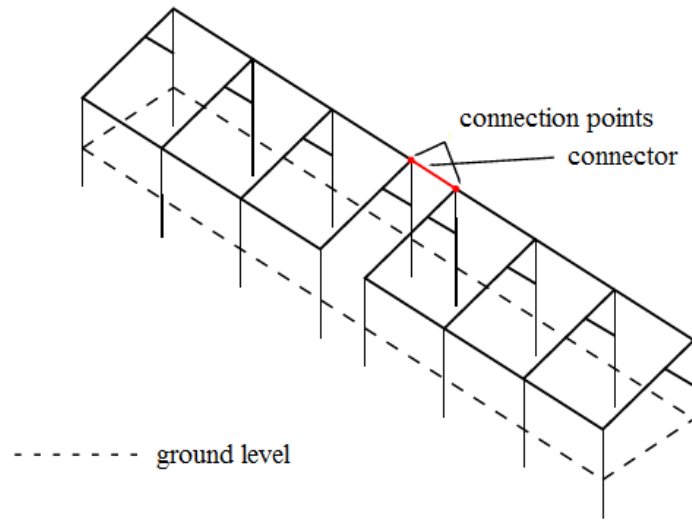
Fig. 3. Sketch of the implementation of connecting supporting tables for photovoltaic modules

not meeting the requirements for direct contact with the lightning discharge channel. In the practice of protecting standalone photovoltaic installations, two methods of mounting lightning rods are most often used: first as free-standing, which means they are separated from the table structure and second as directly attached to the table structure. These two configurations are shown in Fig. 4.
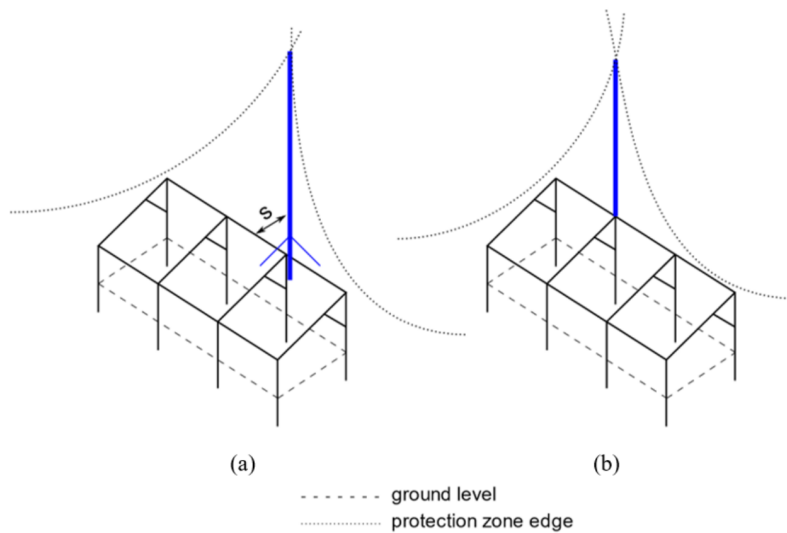

Fig. 4. Visualization of the location of lightning rods: (a) placed next to the supporting table; (b) mounted on the supporting table. The designation s is the minimum separation distance calculated by [6]

The use of separate lightning rods means that they are placed next to the support table at a distance that meets the minimum separation distance requirement calculated according to standard [6], but at least $s = 0.5$ m [7] is recommended, which minimizes the risk of sparking on the protected structure. This solution has both positive and negative effects.

The main positive effect is moving the risk of lightning current away from the table structure because it will flow directly to the earthing system. Due to the galvanic connection of the earth electrode with the tables, the potential of the entire structure will increase its value, and a partial lightning current will flow through the whole structure. In the case of a stand-alone installation, it is impossible to fully separate the lightning protection system from the photovoltaic structure – in each case, there will be an electric path for the current flow through the ground. Such increased distance, however, may reduce the risk of hazardous voltages induced in the cabling of the DC installation connecting the panels with the inverter, or the AC connecting the inverter with the loading part of the installation.

The negative effects are mainly related to the isolation of the lightning rod. Such a lightning rod usually has only one down-conductor connected to the grounding system. The interruption of this path causes a loss of control over the electric path of the lightning current flow and the lightning protection will not function properly. Moreover, a solution with a distanced lightning rod will require a greater number of lightning rods and a specific spacing between the lightning rod and the support table structure. This may involve the need to redesign the arrangement of tables with photovoltaic modules and cause difficulties in the subsequent operation of the farm, e.g., collisions with communication routes. In addition, the shading effect of PV modules may appear because of an increasing number of lightning rods. It involves the necessity to fix the lightning rods on masts placed on the ground so that the protection zone covers the adjacent tables with modules. Consequently, it reduces the efficiency of the solar farm by switching off subsequent rows of modules. Shutting down rows of modules can be a secondary source of problems with the flow of current through the string inverter. Due to the lack of electricity generation, the modules become receivers, which overcharges the inverter and leads to its complete shutdown, disabling all supported rows of modules.

4. Fundamental model

The above assumptions formed the basis for the creation of the fundamental model for further simulation analysis. Computer simulations were performed in the ANSYS/Maxwell 3D environment, and their stages were related to the following elements of the lightning protection system, i.e., lightning rods, down-conductors, the grounding system, as well as induced voltages. The current with peak value $I_m = 40$ kA that led to the upper end of the concerned lightning rod (Fig. 5) was defined as a source of lightning current.

Additionally, the tables were equipped with an integrated lightning rod 1 or a free-standing lightning rod 2 located 1 m next to the left pair of tables. The simulations carried out during this research were based on static magnetic and electric fields. This assumption results from the simplification of the models and the reduction of the calculation time. On the other hand, the aim was to obtain the maximum values of the expected results, hence it can be concluded that this simplification is not a source of a significant error. The whole structure was placed in the air
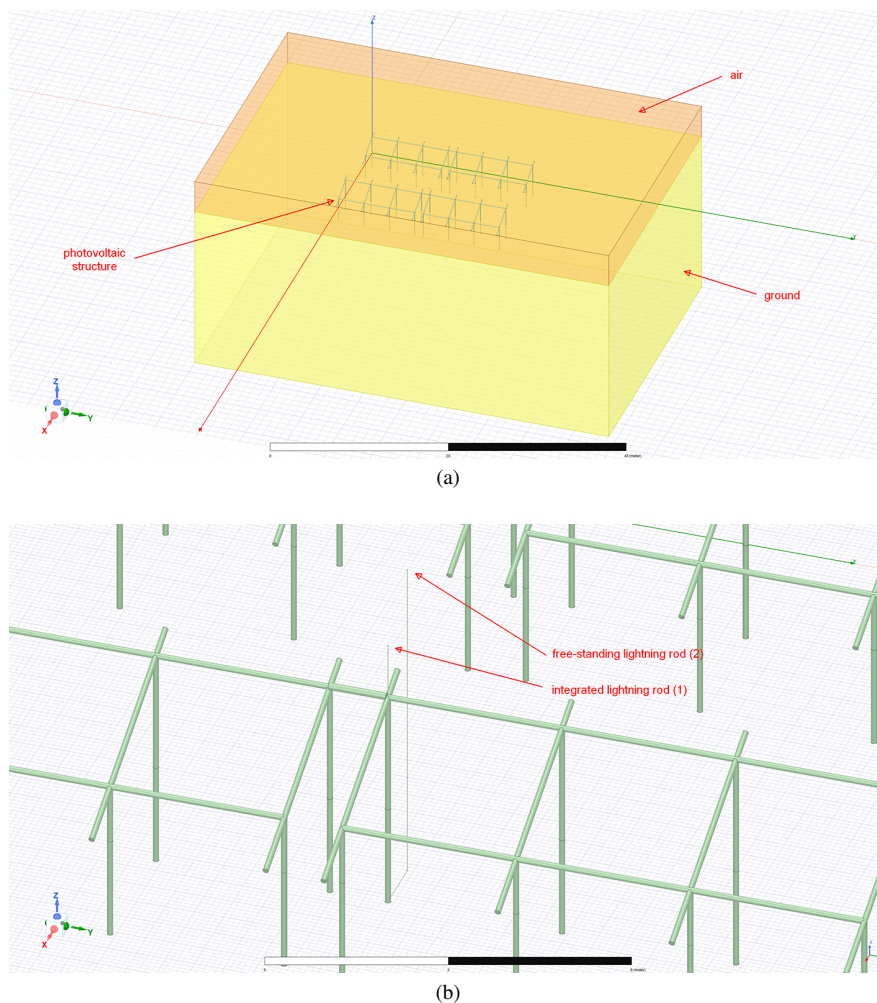
(a)

(b)

Fig. 5. Basic form of simulation model: (a) general form of the model; (b) zoom on two configurations
of lightning rods

and on the ground with a resistivity of $\rho = 200$ Ωm. The bottom ends of the tables' legs were
connected to a mesh grounding, constituting an extensive lattice earth electrode, covering the
entire surface of the photovoltaic power plant. The spacing of the horizontally placed iron band
was $d = 20$ m.

The magnetostatic field simulator solves the magnetic vector potential $A_z(x, y, z)$ in field
Eq. (1):

$$J_z(xyz) = \nabla \times \left(\frac{1}{\mu_r \mu_0} \left(\nabla \times A_z(x, y, z) \right) \right),$$ (1)

where:

- $A_z(x, y, z)$ is the z component of the magnetic vector potential,
- $J_z(x, y, z)$ is the DC current density field flowing in the direction of transmission,
- μ_r is the relative permeability of each material,
- μ_0 is the permeability of free space.

Given $J_z(x, y, z)$ as an excitation, the magnetostatic field simulator computes the magnetic vector potential at all points in space. The equation that the magnetostatic field solver computes is derived from Ampere's law described by Eq. (2):

$$\nabla \times \left(\frac{1}{\mu_r \mu_0} \nabla \times A \right) = J. \tag{2}$$

The magnetostatic field simulator solves this equation using the finite element method. After $A_z(x, y, z)$ is computed, the magnetic flux density B and the magnetic field H can be computed using the relationships $B = \nabla \times A$ and $H = \frac{B}{\mu_r \mu_0}$.

In the case of the electrostatic field simulator, the equation that solves the electric potential $\phi(x, y, z)$ is as in field Eq. (3):

$$\nabla \cdot (\varepsilon_r \varepsilon_0 \nabla \phi(x, y, z)) = -\rho, \tag{3}$$

where:

- $\phi(x, y, z)$ is the electric potential,
- ε_r is the relative permittivity,
- ε_0 is the permittivity of free space,
- $\rho(x, y, z)$ is the charge density.

Equation (3), which the electrostatic field simulator solves using the finite element method, is derived from Gauss's law and from Faraday's law of induction. After the solution for the potential is generated, the system automatically computes the E-field and D-field using the relations $E = -\nabla \phi$ and $D = \varepsilon_r \varepsilon_0 E$.

5. Partial lightning current density results

The first of the obtained simulation results were current density near conducted parts of the supporting table for the configuration with a free-standing lightning rod and integrated with the table. The structures are shown in Fig. 6.

By analyzing the results obtained from the simulations one might conclude that the values of lightning current density distributions flowing between the grounding system sections in both configurations are close to each other. The significant difference is that in the case of separate lightning rods, the highest current density occurs in the connection between the lightning rod and the grounding system. In contrast, in the lightning rod attached to the table structure, this current spreads over several paths, which reduces its density proportionally. These differences may, in practice, convert into a higher probability of electrodynamic forces that may damage the joints of conductive elements.
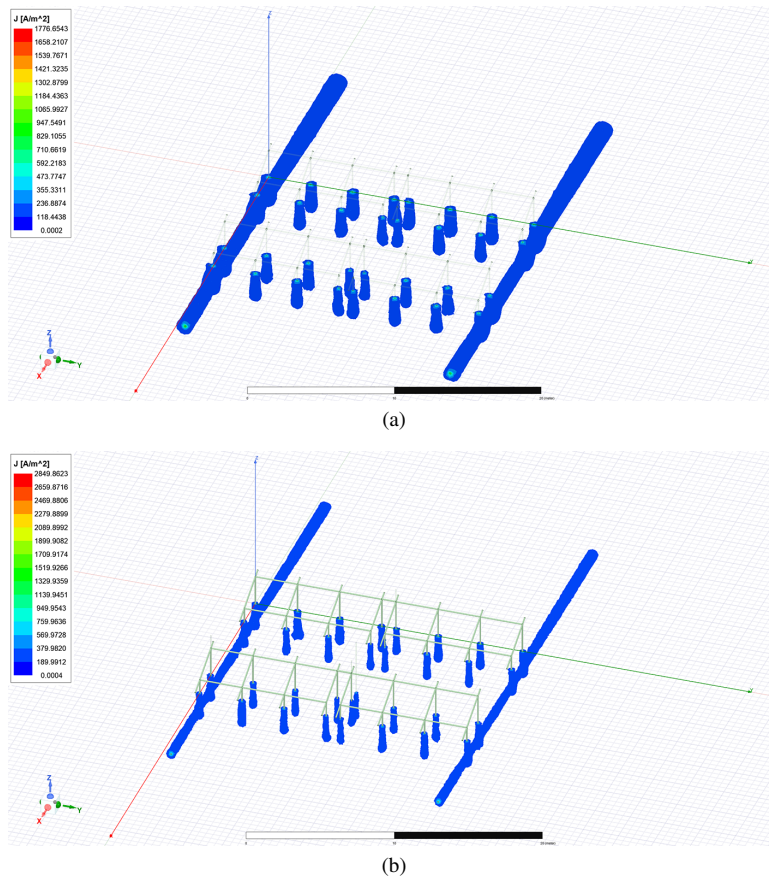
Fig. 6. The lightning current density distribution around conductors below ground level for the configuration: (a) lightning rod attached to the support table structure; (b) lightning rod mounted separate to the support table structure

6. Distribution of lightning current results

The role of down-conductors is to conduct the lightning current from the lightning rod to the grounding system. To reduce the probability of its damage due to the lightning current flowing through the lightning protection system, it should be arranged in such a way that there are several parallel current paths as short as possible from the point of a lightning strike to the ground [6]. The down-conductors might also be conductive components of the photovoltaic farm (natural down-conductors), and conductors used only for lightning protection (artificial down-conductors). The possibility of using the supporting structure of photovoltaic modules is primarily due to its resistance to the expected surge current of a significant peak value. During the simulation tests, the influence of placing the lightning rod on the supporting table structure and as a standalone element was investigated. The distribution of magnetic field strength around the conductive structures was also observed.

The results obtained in these tests are shown in Fig. 7. Extremely high values of field strength marked by red arrows are the result of imperfect geometry in the shape of sharp edges of the model on the mesh grid. As it may be observed, the values of magnetic field strength were much smaller in the case of the direct lightning strike to the lightning rod integrated with the supporting table. This fact may be explained due to lightning current distribution into more conducted paths than in the case of separated lightning rods. Lower values of lightning current lead to lower values of magnetic field strength and lower values of induced voltages.

(a)

(b)
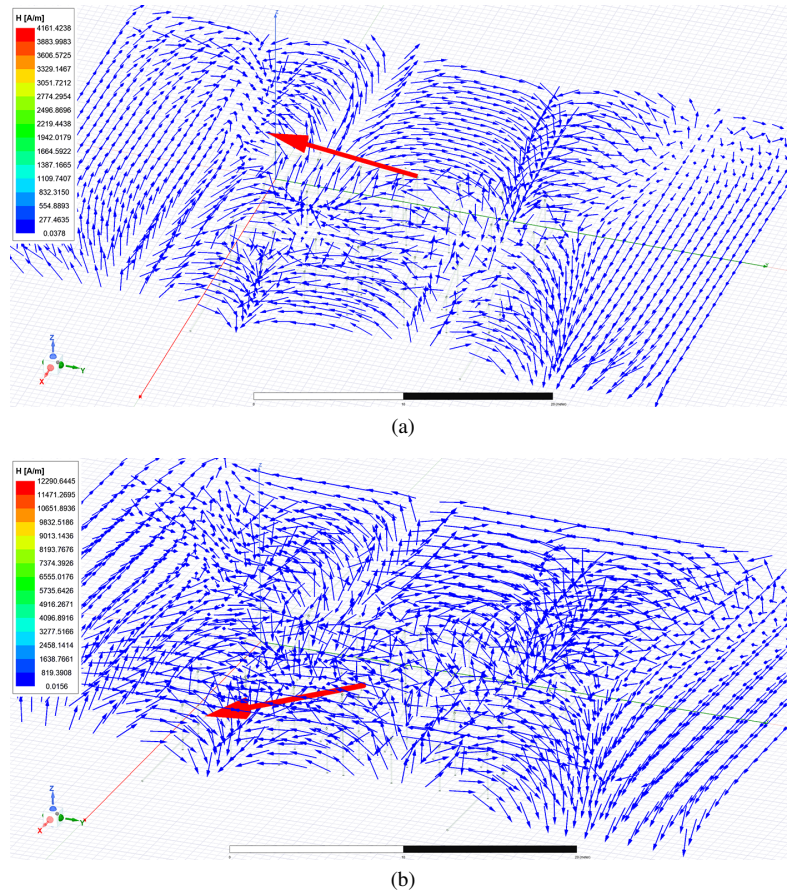
Fig. 7. Exemplary results of vector magnetic field distribution in case of direct lighting strike to lightning rod: (a) integrated with supporting table; (b) separated to supporting table

7. Grounding system

The grounding system performs an extremely important role in the lightning protection system because it should safely disperse the lightning current in the ground. Its parameters must meet the requirements for the functions it performs throughout the life of the installation. For

lightning protection applications the grounding system should be made following the normative requirements presented in the lightning protection standard EN 62305 [5, 6, 8, 9]. However, one should remember the discrepancies resulting from the separate development of various standards for designing grounding systems for extensive photovoltaic installations. An example may be the recommendation to make a lattice earth electrode with a mesh size from 20×20 m to 40×40 m by the standard of [7], while the standard of [10] recommends making a horizontal earth electrode for each table (Fig. 8).

(a)

(b)
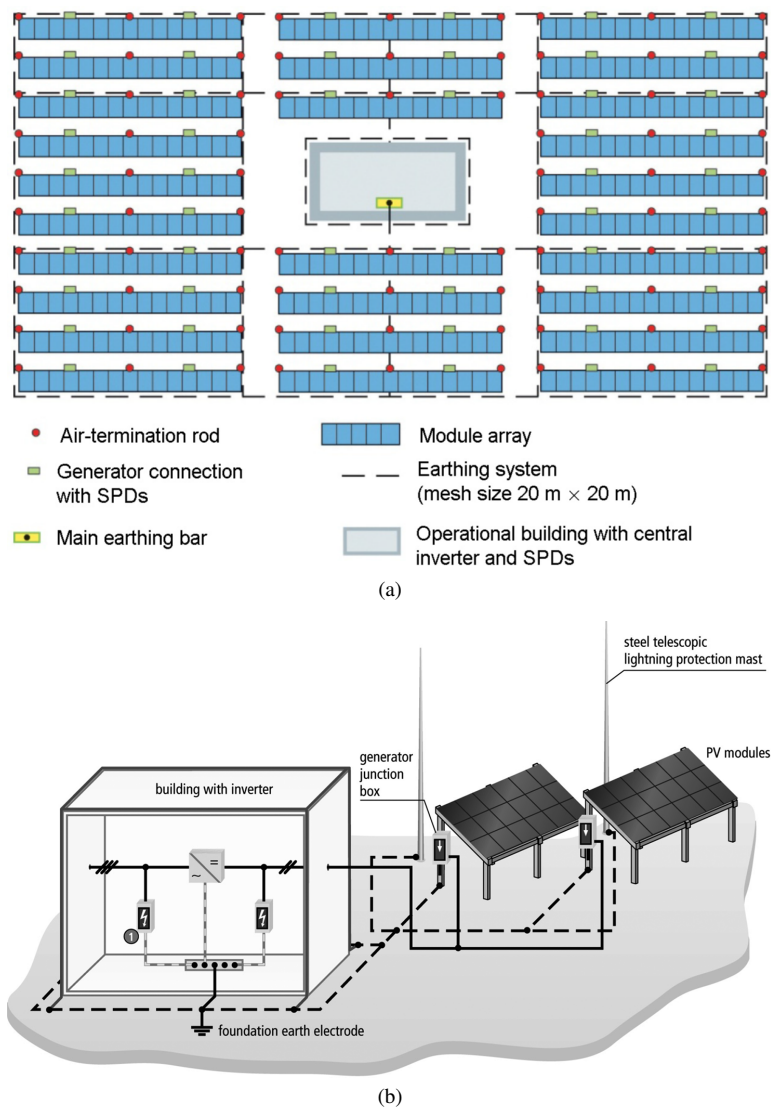
Fig. 8. An example of ambiguous requirements regarding the type of ground electrode of a ground-based photovoltaic installation: (a) according to [7]; (b) according to [10]

The flow of current through the earth electrodes causes a voltage drop on the conductive earthing elements, and consequently, an electric field is created. The distribution of the potential on the ground surface depends on the geometric dimensions and shape of the earth electrode and the geoelectric properties of the soil, mainly the soil resistivity ρ and its layered structure [11,12]. Due to such ambiguities, a frequent practical question is how to make an earth electrode for such a structure and its dimensions. Hence, three configurations were selected for simulation tests:

– only table legs placed into the ground,
– a horizontally placed iron band at one end of a row of tables,
– horizontally placed iron band at both ends of a row of tables.

The solution follows [10] and is optimal both in terms of electrical safety as well as economic and technical issues, it is understood as the time spent on its construction. An iron band laid along the AC electrical installation channels ensures the equipotentiality of the ground along its path, minimizing the occurrence of significant potential differences and partial discharges, which are the cause of insulation breakdown and overvoltage. The cross-sectional area of the iron band should comply with the requirements set out in Table 7 of the standard [6]. The theoretical considerations were visualized using the model presented in Fig. 5 with the additional horizontally placed iron band in the subsequent stages of the research. A lightning current of $I = 40$ kA and a soil resistivity of $\rho = 200$ Ωm were assumed as sources of the threat. The exemplary results are show in Figs. 9–11.

The simulations might be stated that the configuration with an iron band placed at both ends of the tables is the optimal solution and lightning rod attached to supporting structure. The basis for such a conclusion is the fact that for such a configuration the smallest peak values of the electrical potential on the surface of the earth are observed, as well as noticeably lower values of step voltages. An issue that should be considered individually due to the structure and electrical parameters of the soil is the maximum spacing of iron band conductors. It should be also remembered that it is essential to maintain the continuity of the installation by making the correct connections following standard requirements [13], the best confirmed by electrical measurements in the field of galvanic continuity.
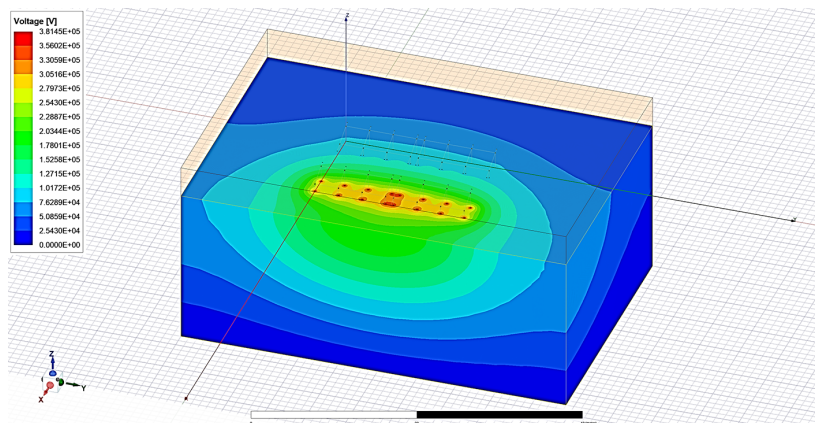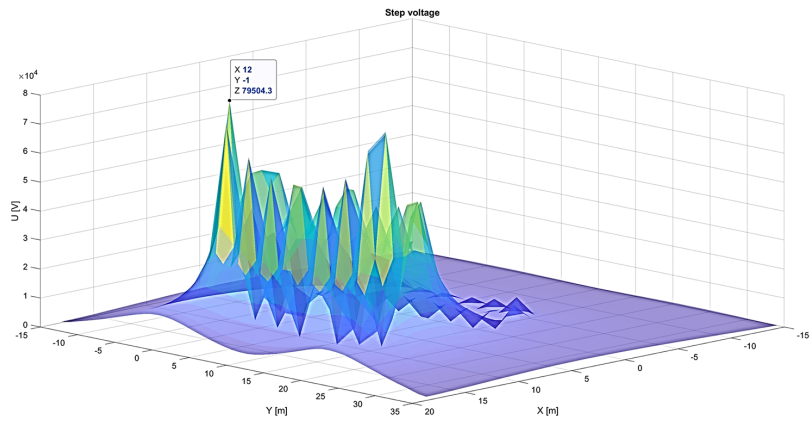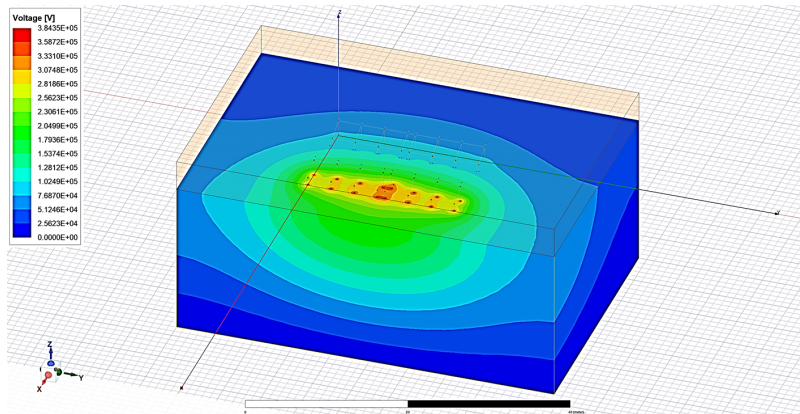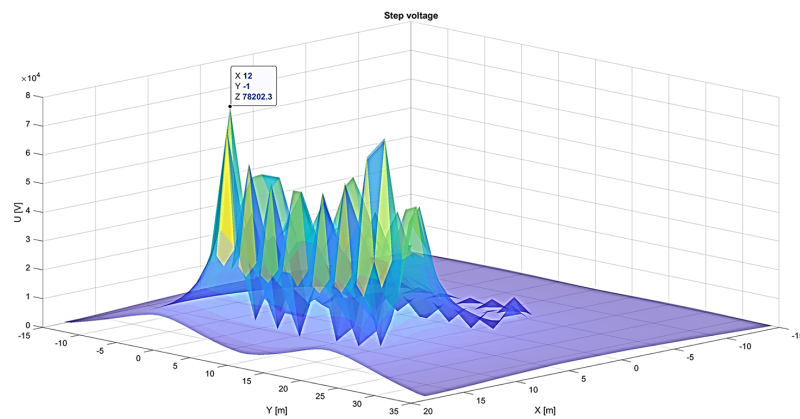

Fig. 9(a) surface potential for direct hit to integrated lightning rod

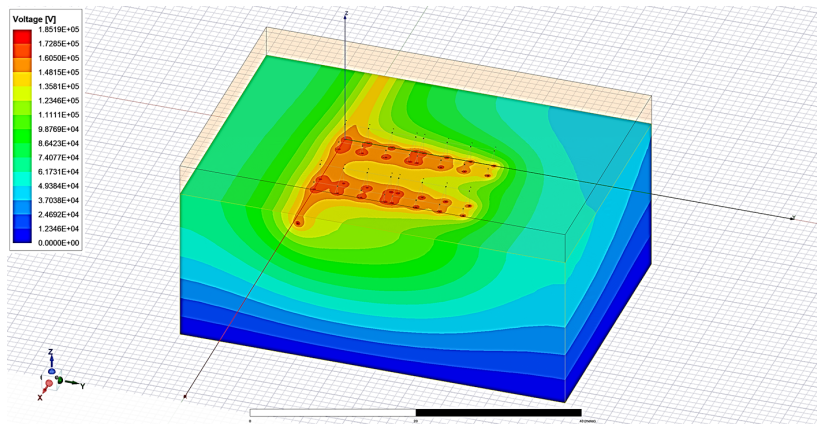(b) step voltage for direct hit to integrated lightning rod

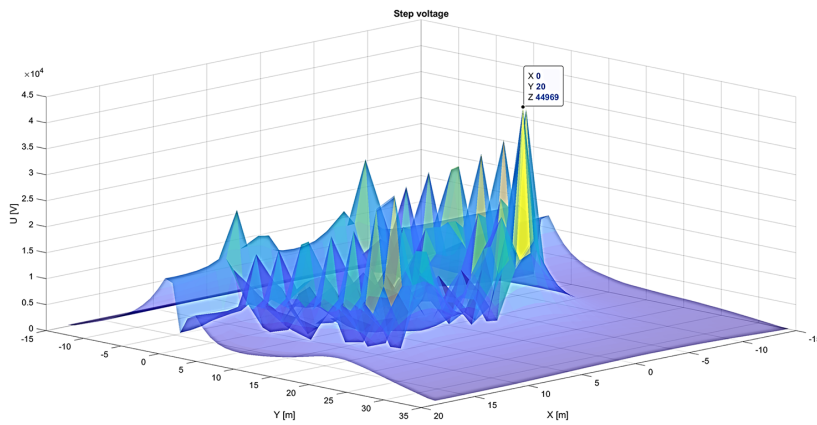(c) surface potential for direct hit to standalone lightning rod

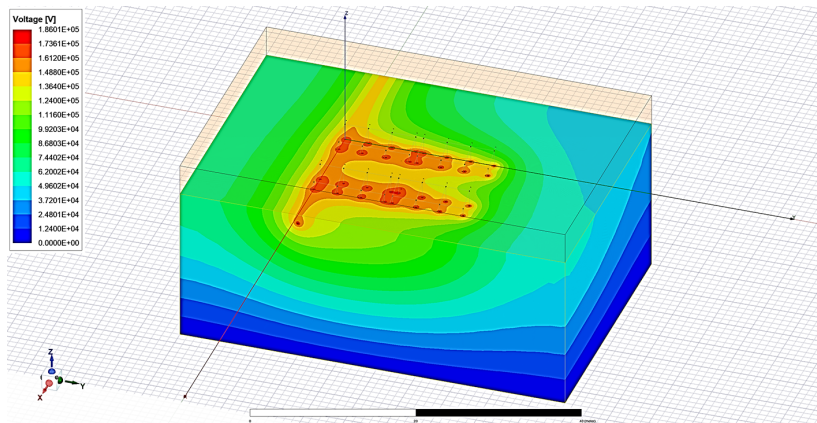(d) step voltage for direct hit to standalone lightning rod

Fig. 9. Simulation results for four tables connected in pairs in parallel

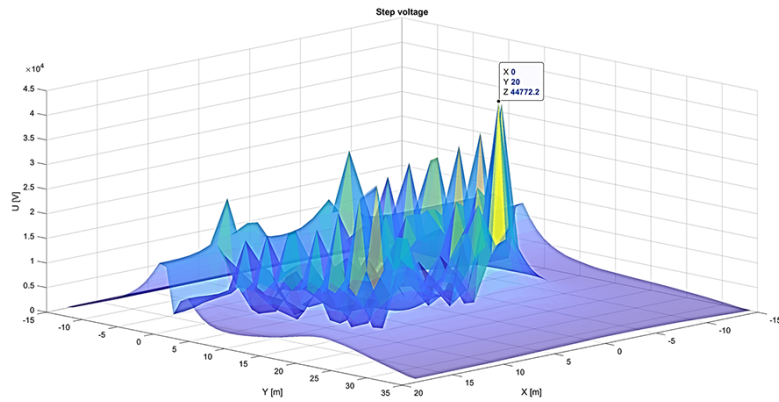(a) surface potential for direct hit to integrated lightning rod

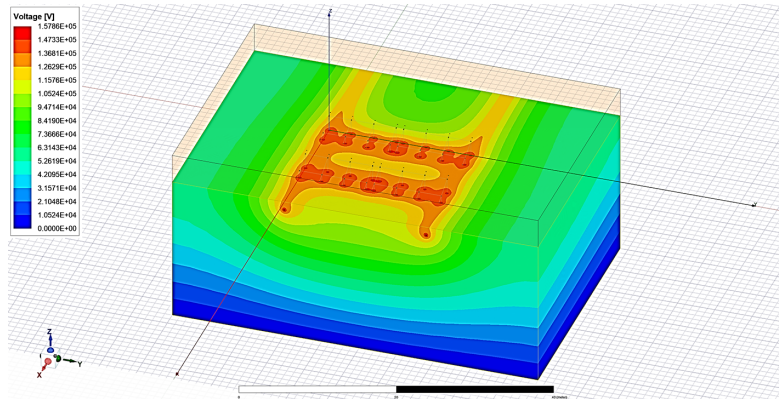(b) step voltage for direct hit to integrated lightning rod

(c) surface potential for direct hit to standalone lightning rod
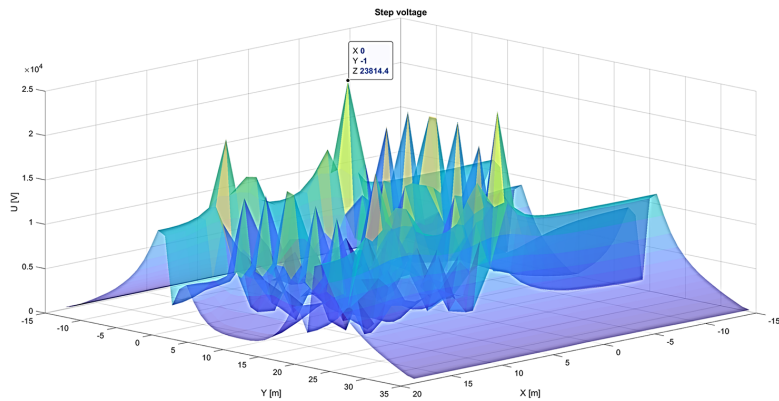
Fig. 10(a)–(c)

(d) step voltage for direct hit to standalone lightning rod

Fig. 10. Simulation results for four tables connected in parallel in pairs and a horizontally placed iron band at one end of the tables
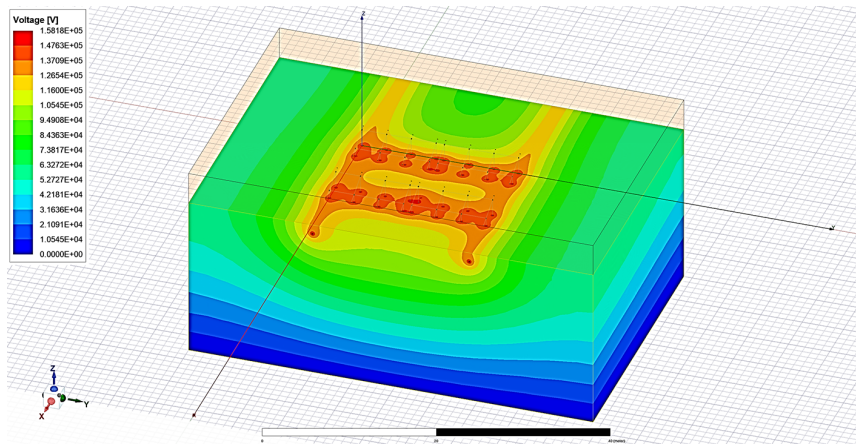

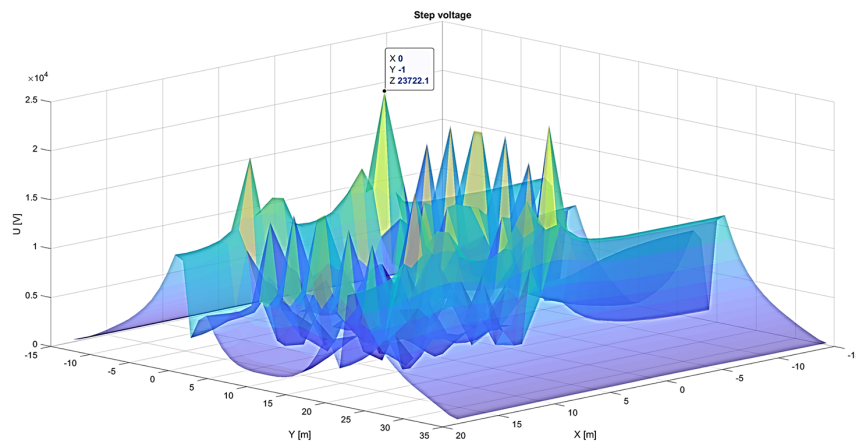(a) surface potential for direct hit to integrated lightning rod

(b) step voltage for direct hit to integrated lightning rod

Fig. 11(a), (b)

(c) surface potential for direct hit to standalone lightning rod

(d) step voltage for direct hit to standalone lightning rod

Fig. 11. Simulation results for four tables connected in parallel in pairs and a horizontally placed iron band at both ends of the tables

To improve the visualization part of the real installation, an extended simulation was performed for the configuration consisting of 16 tables organized in two rows by eight tables in each of them with the use of an earthing iron band placed transversely to the rows of the tables at their ends, which resulted in a spacing $d = 80$ m.

According to the simulation presented in Fig. 12, it can be concluded that the potential values have decreased significantly. This result is due to the lightning current that flows to the ground through a much greater number of conductive connections and a much larger current dissipation area in the ground. Step voltages have also noticeably decreased in their value, which has increased the safety of using such a photovoltaic power plant.
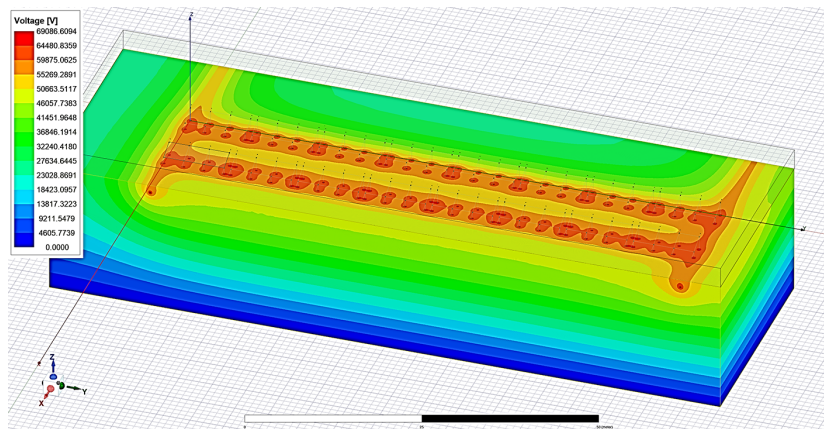
(a)
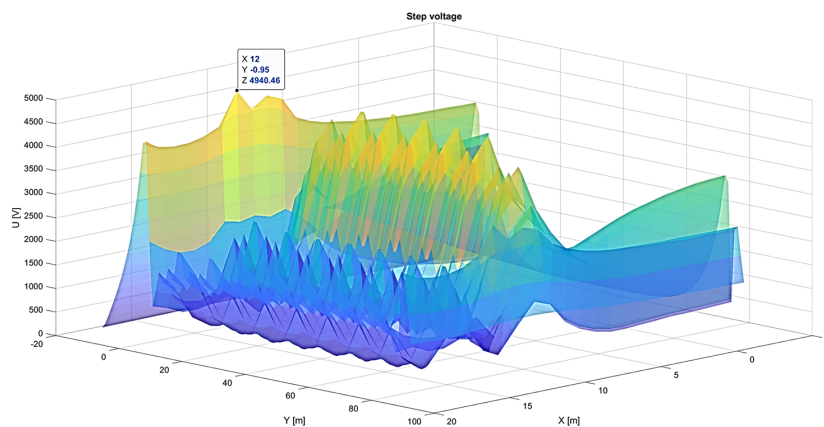
(b)

Fig. 12. Simulation results for 16 tables, 80 meter iron band spacing and 40 kA discharge to lightning rod integrated with the table structure: (a) surface potential; (b) step voltage

8. Induced voltages

The value of the induced voltage depends on such factors as the value of the magnetic flux penetrating the conductive loop formed, for example, by the wires of the electrical installation, the surface of this loop, its arrangement relative to the magnetic flux vector and the speed of its change (steepness). While we have little influence on the value of the flux and the speed of its change, in practice, it is possible to take action to minimize the surface of conductive loops or protect it by measures like surge protection devices. This is an important issue because both the peak values of the lightning current as well as the speed of its changes are significant. Since the flux of the magnetic field is directly proportional to the current that causes it, hence its parameters will be equally critical.

The process at which the magnetic field $B(t)$ of a lightning discharge passes through conductor loops is referred to as magnetic field coupling or magnetic induction (Fig. 13). If the conductor loops are open, the voltages u_{ind} will result in proportion to dB/dt, however, where the conductor loops are short-circuited, the currents i_{ind} will result in proportion to $B(t)$ and the value of conducted structure impedance. Assuming the worst-case scenario when a conductive loop has the largest surface and covers the entire table (Fig. 14), the following results were obtained.
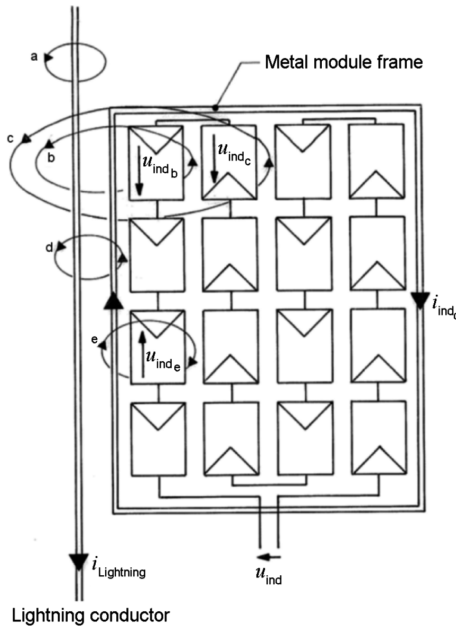

Fig. 13. Example geometry related to voltage induction in the installation
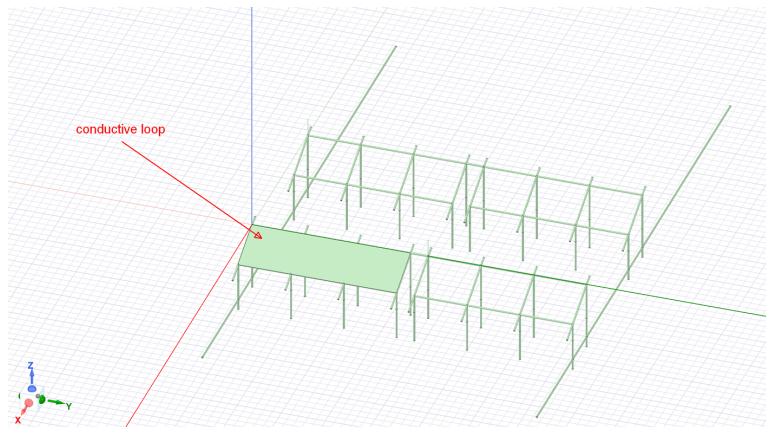of a photovoltaic module [7]

Fig. 14. Model for the calculation of the induced voltage

The calculations were made also in the ANSYS environment according to Formula (4):

$$U_n = -\frac{\mathrm{d}}{\mathrm{d}t} \int_S B\,\mathrm{d}S.$$ (4)

Since the simulation was performed in a static domain, it was necessary to assume the speed of change in the flux over time, which value was assumed to be $\mathrm{d}t = 1$ µs. Only the component perpendicular to the conductive surface was considered in the calculations. The value of the conductive loop area in the assumed case was $S = 23.751$ m^2.

The induced voltage for lightning discharge to a stand-alone lightning rod was $U_{i1} = 32.2$ kV, but for hitting a lightning rod integrated with the table structure, it was $U_{i2} = 28.3$ kV. On the one hand, the obtained results may be surprising because in the configuration with the integrated lightning rod, the lightning strike is located closer to it than in the configuration with the stand-alone lightning rod. On the other hand, the magnetic field strength depends on the intensity of the current, and because of the greater number of paths, it is smaller in the configuration with the integrated lightning rod. Nevertheless, it should be noted that in this situation lightning current flows through the table structure, therefore, special attention should be paid to the proper selection of construction materials and all fixings, so that thermal and mechanical damage does not occur due to the flow of the lightning current of considerable value and dynamics. In both cases, it is clearly visible that it is advisable to install appropriately selected surge limiting devices in each installation.

9. Conclusion

Based on the simulation tests performed, it can be concluded that:

1. Mounting a lightning rod integrated with the table results in higher values of current flowing through the table structure. As a result, it is more exposed to electrodynamic and electrothermal influences. Hence, in such a configuration, it is recommended to pay special attention to selecting construction materials and the quality of connections.

2. Installing a separated lightning rod causes an increased value of magnetic field strength around the table structure, which translates into higher values of induced voltages in electrical installations and also in conductive loops created by part of electrical installations and supporting structure. It is very important to route cables to minimize their loop area. It is one of the easiest ways to minimize dangerous induced voltages.

3. The influence of the method of assembling the lightning rod on the distribution of the electric potential on the earth's surface is negligible. The obtained values were very similar in each case.

4. Installing an additional iron band in the direction perpendicular to the table line decreases the maximum values of the electric potential on the earth's surface. It also minimizes dangerous values of step voltages on the earth's surface.
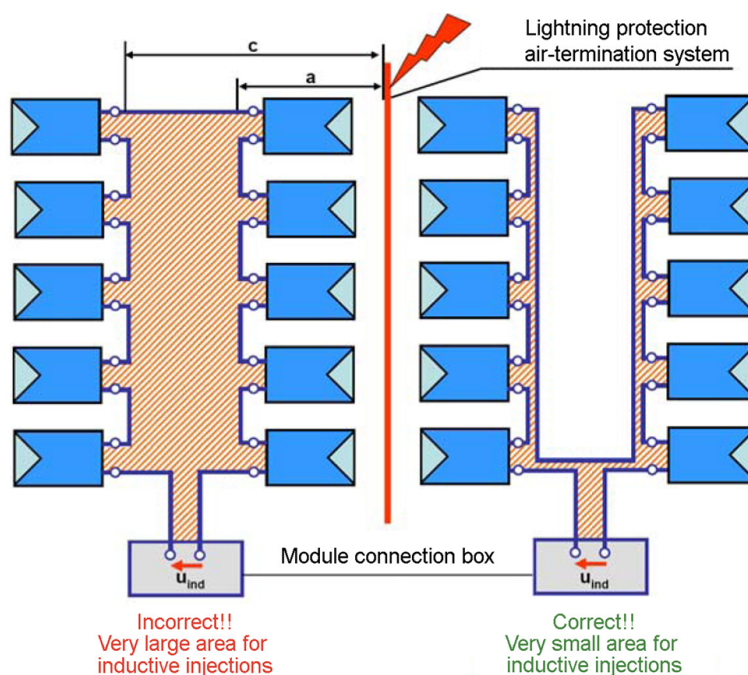
Fig. 15. Reduction of the effects of induction by line routeing [7]

References

[1] Bielec-Bąkowska Z., *Storms and hail in Poland*, Institute of Geography and Spatial Management – Jagiellonian University in Kraków, Geographic Works (in Polish), no. 132, Cracow (2013).

[2] Carrascal H.O., *NTC vs IEC: Comparative analysis between the lightning protection standards: NTC 4552 and IEC 62305 using a practical example*, 2014 IEEE ANDESCON (2014), DOI: 10.1109/AN-DESCON.2014.7098552.

[3] Sobieska E., Sobolewski K., *Modelling and simulation of lightning protection systems for facilities equipped with a photovoltaic installation*, Computational Problems of Electrical Engineering (in Polish), Warsaw, Poland (2020), DOI: 10.15199/48.2021.06.16.

[4] Zhang Y., Chen H., Du Y.P., *Lightning protection design of solar photovoltaic systems: Methodology and guidelines*, Electric Power Systems Research 174 (2019), DOI: 10.1016/j.epsr.2019.105877.

[5] PN-EN 62305-1:2011, *Protection against lightning. Part 1: General principles* (2011).

[6] PN-EN 62305-3:2011, *Protection against lightning. Part 3: Physical damage to structures and life hazard*, (2011).

[7] IEC TR 63227:2020, *Lightning and surge voltage protection for photovoltaic (PV) power supply systems* (2020).

[8] PN-EN 62305-2:2012, *Protection against lightning. Part 2: Risk management* (2012).

[9] PN-EN 62305-4:2011, *Protection against lightning. Part 4: Electrical and electronic systems within structures* (2011).

[10] PN-HD 60364-7-712:2016-05, *Low-voltage electrical installations. Part 7-712: Requirements for special installations or locations – Photovoltaic (PV) systems* (2016).

[11] Sobolewski K., *Modeling and simulations in the earthing calculations*, Computational Problems of Electrical Engineering, Slavsko, Ukraine (2019), DOI: 10.1109/CPEE47179.2019.8949132.

[12] Łukaszewski A., Nogal Ł., *Influence of lightning current surge shape and peak value on grounding parameters*, Bulletin of the Polish Academy of Sciences: Technical Sciences, vol. 69, no. 2 (2021), DOI: 10.24425/bpasts.2021.136730.

[13] PN-EN 62561-1:2017-07, *Lightning Protection System Components (LPSC). Part 1: Requirements for connection components* (2017).

[14] Furado F., Vidal P., Hernandez J., *Lightning and Surge Protection in Photovoltaic Installations*, Power Delivery, IEEE Transactions on Power Deliver, vol. 23, iss. 4, pp. 1961–1971, DOI: 10.1109/TP-WRD.2008.917886.

[15] Cooper M.A., Holle R., *Lightning Protection*, Springer Natural Hazard (2019).

[16] Tan P.H., Gan C.K., *Methods of lightning protection for the PV power plant*, 2013 IEEE Student Conference on Research and Developement (2013), DOI: 10.1109/SCOReD.2013.7002575.

[17] Gomes A., Gomes C., Ab Kadir M.Z.K., Izadi M., Rock M., *Evaluation of lightning protection systems proposed for small structures by electromagnetic simulation*, 2016 33rd International Conference on Lightning Protection (ICLP) (2016), DOI: 10.1109/ICLP.2018.8503276.

[18] Christodoulou C.A., Ekonomou L., Gonos I.F., Papanikolaou N.P., *Lightning protection of PV systems*, in Energy Systems (2016), DOI: 10.1007/s12667-015-0176-2.

[19] Charalambous C.A., Kokkinos N.D., Christofides N., *External Lightning Protection and Grounding in Large-Scale Photovoltaic Applications*, IEEE Transactions on electromagnetic compatibility (2013), DOI: 10.1109/TEMC.2013.2280027.

[20] Damianaki K., Christodoulou C.A., Kokalis C.-C.A., Kyritsis A., Ellinas E.D., Vita V., Gonos I.F., *Lightning Protection of Photovoltaic Systems: Computation of the Developed Potentials*, Applied science (2020), DOI: 10.3390/app11010337.